Tunable Mie-Resonant Dielectric Metasurfaces Based on VO2 Phase-Transition Materials

Aditya Tripathi, Jimmy John, Sergey Kruk, Zhen Zhang, Hai Son Nguyen, Lotfi Berguiga, Pedro Rojo Romeo, Régis Orobtchouk, Shriram Ramanathan, Yuri Kivshar, et al.

Tunable Mie-resonant dielectric metasurfaces based on VO_2 phase-transition materials

Aditya Tripathi[1], Jimmy John[2], Sergey Kruk[1], Zhen Zhang[3], Hai Son Nguyen[2,4], Lotfi Berguiga[2], Pedro Rojo Romeo[2], Régis Orobtchouk[2], Shriram Ramanathan[3], Yuri Kivshar[1] and Sébastien Cueff[2]

[1]Nonlinear Physics Centre, Research School of Physics, Australian National University, Canberra ACT 2601, Australia
[2] Université de Lyon, Institut des Nanotechnologies de Lyon (INL) UMR 5270 CNRS, École Centrale de Lyon, 69134, Ecully, France
[3]School of Materials Engineering, Purdue University, West Lafayette, IN 47907, USA
[4]Institut Universitaire de France (IUF)
Author e-mail address: sebastien.cueff@ec-lyon.fr

ABSTRACT: Dielectric metasurfaces have become efficient tools for creating ultrathin optical components with various functionalities for imaging, holography, quantum optics, and topological photonics. While static all-dielectric resonant metaphotonics is reaching maturity, challenges remain in the design and fabrication of efficient reconfigurable and tunable metasurface structures. A promising pathway towards tunable metasurfaces is by incorporating phase-transition materials into the photonic structure design. Here we demonstrate Mie-resonant silicon-based metasurfaces tunable via the insulator-to-metal transition of a thin VO_2 layer with reversible properties at telecom wavelengths. We experimentally demonstrate two regimes of functional tunability driven by the VO_2 transition: (i) two orders of magnitude modulation of the metasurface transmission, (ii) spectral tuning of near-perfect absorption. Both functionalities are accompanied by a hysteresis-like behavior that can be exploited for versatile memory effects. Beyond this demonstration of multifunctional properties, this work provides a general framework to efficiently use the full complex refractive index tuning of VO_2, both for its refractive index modulation and optical absorption tuning. Tunable dielectric metasurfaces may find their applications in various photonics technologies including optical communications, information storage, imaging, detectors, and sensors.

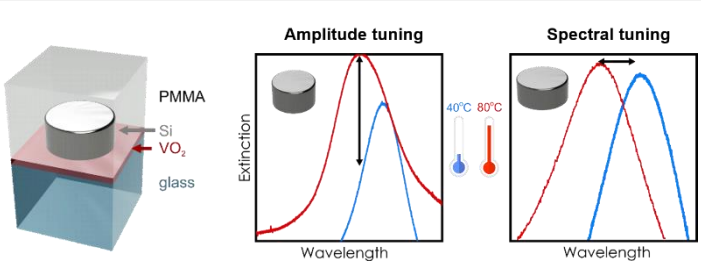

KEYWORDS: *Metasurfaces, phase-change materials, vanadium dioxide, tunable nanophotonics, spectral modulation, near-infrared*

Introduction

Metasurfaces have emerged as a flexible and efficient platform for manipulating electromagnetic waves. In particular, recent demonstrations of Mie-resonant nanostructures made of high-index dielectric materials opened up exciting opportunities to tailor the phase, amplitude and polarization of scattered light through designer multipolar resonances.[1,2] Such dielectric resonators, assembled to form metasurfaces, provide a considerable design space for the control of both electric and magnetic fields with low material losses as well as CMOS compatibility for large-scale manufacturing. Employing multipolar resonances in metasurfaces therefore provides novel strategies for creating compact optical devices for various applications ranging from optical sensing to holography or quantum optics.

Today static dielectric metasurfaces such as metalenses or other flat optics match the performance or outperform conventional optical elements[3] and current research agenda has shifted from fundamental concepts to applied research and applications.[4] The future expansion of this technology towards practical photonic devices requires developing tunable metasurfaces platforms.[5,6] However, design and fabrication of reconfigurable and tunable metasurfaces imposes a few challenges. Several pathways towards tunable metasurfaces have been explored in the literature, including mechanical deformations of the metasurfaces' substrates,[7,8] liquid crystals infiltration,[9,10] free charge carrier density variation,[11,12] ultrafast nonlinear response,[13,14] as well as incorporation of phase-change[15] and phase-transition materials into the device.[16]

During recent years, we have seen a rapid progress in the development of tunable metasurfaces based on GST materials (germanium-antimony-tellurium or GeSbTe) which are phase-change materials from the group of chalcogenide glasses used in rewritable optical disks and phase-change memory applications.[17] Recent demonstrations of such metasurfaces include reconfigurable flat optical components enabling the control of either the amplitude or phase of reflected/transmitted fields,[18-21] beam-steering,[22] free-space modulators with multi-level control,[23,24] tunable spectral filters,[25] tunable metalens[26] and programmable Huygens' metasurfaces.[27]

However, some of the limitation of GST include the volume expansion, surface oxidation and surface roughness creation accompanying the amorphous-to-crystalline transition. In addition, the intense pulsed lasers needed for its re-amorphization

(reset) may exceed laser damage threshold of the surrounding materials.

These limitations are mitigated in another class of tunable metasurfaces, based on correlated electron phase-transition materials such as vanadium dioxide (VO_2).[16,28-33] VO_2 is a particularly attractive phase-transition material whose dynamical change of phase corresponds to a subtle crystalline–to–crystalline transition and is therefore not accompanied by catastrophic fracture or void creation in thin films.[34,35] The transition can be triggered optically, electrically or thermally at temperatures close to ambient (~68°C). Switching VO_2 is therefore versatile, easy to control and its state is naturally reset when the excitation is off. For these reasons, VO_2 is of interest for hybrid integration with materials and/or technologies that cannot support intense pulsed lasers or high temperatures for device operation.

The exceptionally large complex refractive index variation produced by the insulator-to-metal transition of this material opens interesting opportunities to dynamically tune optical systems. Several works on VO_2-based metasurfaces reported to date rely on metallic antennas integrated on VO_2 thin films.[32-35] However, efficiencies of metal-based designs remain limited by absorption losses and relatively weak magnetic Mie resonances. In contrast, all-dielectric designs for resonant elements hold promise to significantly advance reconfigurable metasurfaces. However nanofabrication of hybrid VO_2-dielectric metasurfaces remains largely premature. Very recently first examples of hybrid VO_2-Si metasurfaces have been demonstrated.[16,36] In ref. 16, Howes et al. employed bi-layer Si-VO_2 disks to realise tunable metasurface. Parameters of the metasurface were chosen close to Si-based Huygens' metasurfaces,[37] and the design was further numerically optimised to realise tunable absorption which may find applications in continuously tunable filters and detectors, refractive index sensing, frequency-selective bolometers, solar energy harvester or thermal photovoltaic power generation.[38,39]

In this work, we analyse theoretically and verify experimentally design principles of hybrid dielectric-VO_2 metasurfaces for tunable transmission, reflection and absorption. We adopt widely used design principles for Huygens' metasurfaces[37] and the Kerker effects.[16,40] We further consider tunable amount of absorption loss added by the VO_2 material by incorporating a concept of coherent perfect absorption.[41] We demonstrate that tunable characteristics of metasurfaces become dependent on the balance between radiative and absorptive losses in hybrid VO_2-Si designs and describe regimes of critical coupling upon which radiative and absorptive losses are balanced enabling near-perfect absorption of light even in metasurfaces with extremely thin layers of semi-absorptive VO_2.

We proceed with the descriptions of the design, fabrication, and characterization of a hybrid dielectric metasurface made of silicon resonators coupled to a layer of VO_2, as presented schematically in Fig. 1. We design the metasurface for the spectral range of fibre telecommunications, however we note that the design wavelength can be tuned widely via adjustments of geometrical parameters. The metasurface is designed to support both electric and magnetic Mie-resonant dipolar modes. Our choice of the spectral and the multipolar range dictates the range of geometrical parameters of the metasurface building blocks. The VO_2 layer is exploited both for its refractive index tuning – to modulate the Mie-resonances – and for its extinction coefficient tuning – to provide an extra degree of freedom for reconfiguring the out-coupling channels. The phase state of the VO_2 layer hence governs the interaction between the incident light and the two resonant modes. To highlight the significant design flexibility and multifunctional features, we demonstrate two different regimes of reversible tuning operation with a same platform: (i) demonstration of a dynamic switch from a Huygens' metasurface to a coherent perfect absorption with a two orders of magnitude amplitude modulation; (ii) demonstration of a spectrally tunable near-perfect absorber.

Results and Discussion

First, we develop simple analytical models for illustrative descriptions of Huygens' metasurfaces and discussion of the scenario of coherent perfect absorption. The operational principle of Huygens' metasurface is based on the excitation of both electric dipole (ED) and magnetic dipole (MD) modes supported by a dielectric Mie-resonant particle. High-index dielectric disks supporting ED and MD resonances may form a translucent array – a Huygens' metasurface – provided both resonances overlap spectrally and have similar amplitude and radiative loss. This phenomenon is also known as the Kerker effect.[40]

The spectral performance of Huygens' metasurfaces can be described phenomenologically within an approximation of the dipoles as Lorentzian oscillators.[37] The frequency-dependent field-transmittance and reflectance can then be written as:

$$t = 1 + \frac{2i\gamma_{\mathrm{ED}}\omega}{\omega_{\mathrm{ED}}^2 - \omega^2 - 2i\gamma_{\mathrm{ED}}\omega} + \frac{2i\gamma_{\mathrm{MD}}\omega}{\omega_{\mathrm{MD}}^2 - \omega^2 - 2i\gamma_{\mathrm{MD}}\omega} \quad (1)$$

$$r = \frac{2i\gamma_{\mathrm{ED}}\omega}{\omega_{\mathrm{ED}}^2 - \omega^2 - 2i\gamma_{\mathrm{ED}}\omega} - \frac{2i\gamma_{\mathrm{MD}}\omega}{\omega_{\mathrm{MD}}^2 - \omega^2 - 2i\gamma_{\mathrm{MD}}\omega} \quad (2)$$

The condition of full transparency requires coincidence of the resonant frequencies $\omega_{\mathrm{ED}} = \omega_{\mathrm{MD}}$ and radiative loss parameters $\gamma_{\mathrm{ED}} = \gamma_{\mathrm{MD}}$. Here the two dipoles are also assumed to have amplitude of 1. The optical features of these resonant dipoles are set both by the geometry of the resonators (shape and dimensions) and by the refractive index of the constituent material. Integrating tunable materials in such metasurfaces would therefore provide a direct means to actively modulate the amplitude and wavelength of the different resonances and therefore modify the transparency condition.

Similar simplistic model may be used to describe absorption in such systems once absorption losses δ_{ED} and δ_{MD} are incorporated in the Lorentz oscillator model,[41] and transmission correspondingly reads:

$$t^{\mathrm{ED}}(\omega) = 1 + \frac{2i\gamma_{\mathrm{ED}}\omega}{{\omega_{\mathrm{ED}}}^2 - \omega^2 - 2i(\gamma_{\mathrm{ED}} + \delta_{\mathrm{ED}})\omega} \quad (3)$$

$$t^{\mathrm{MD}}(\omega) = 1 + \frac{2i\gamma_{MD}\omega}{{\omega_{\mathrm{MD}}}^2 - \omega^2 - 2i(\gamma_{\mathrm{MD}} + \delta_{\mathrm{MD}})\omega} \quad (4)$$

At an additional condition $\gamma_{\mathrm{ED}} = \delta_{\mathrm{ED}}$; and $\gamma_{\mathrm{MD}} = \delta_{\mathrm{MD}}$, i.e. if the absorption loss equals the radiative loss, the metasurface reaches the regime of coherent perfect absorption. Thus, if the absorption loss of the metasurface can be tuned substantially, the metasurface may experience a transition from a Huygens'-like regime to a coherent perfect absorption-like regime. Interestingly, the tunable absorption is one of the characteristic features of VO_2 thin films,

which may therefore be exploited as an additional means to dynamically switch between such regimes.

Therefore, the full complex refractive index modulation of VO_2 (Δn & Δk) may be exploited to design dynamically reconfigurable metasurfaces with various functionalities.

Next, we proceed with the full-wave numerical simulations of metasurfaces consisting of Si disks that host electric and magnetic dipole Mie resonances over a VO_2 layer that serves as a source of tunable refractive index and absorption loss. We design metasurfaces working at around 1.4 μm wavelength having a period of 700 nm, disk height 240 nm, VO_2 thickness 25 nm. The Si disks are separated from the VO_2 layer by a 13 nm thick SiO_2 spacer. We include a SiO_2 spacer in the design, taking into account technological aspects of our nanofabrication approach, namely to protect the VO_2 layer during Si disk fabrication, in particular during the etching processes. Our Si-VO_2 metasurface rests on a glass substrate and it is covered with a layer of PMMA polymer. Similar refractive indices of the glass and the PMMA create a homogeneous optical environment for the metasurface. The complex refractive index of VO_2 in all its phases was extracted from spectroscopic ellipsometry measurements (more details in Refs. 35, 42 and in the Supporting Information). The numerical simulations were performed on COMSOL using Floquet boundary conditions on a unit cell identical to fig 1(a). The full fields and scattered fields were both calculated and used to evaluate transmission and scattering cross-sections respectively. The multipolar decompositions were evaluated using spherical harmonics as described in ref. 43.

We scan disk diameters in the range of 200-650 nm (see Figs. 2a,b), perform multipolar decomposition of their optical response, and find that electric and magnetic dipole modes overlap at around 510 nm diameter (see Fig. 2e). Figures 2f-i show examples of normalized electric field distribution inside the samples for both insulating and metallic phases of the VO_2 layer for disk diameter 550 nm at several different wavelengths ((f) 1410 nm, (g) 1470 nm, (h) 1380 nm and (i) 1450 nm) corresponding to maxima of the electric and the magnetic dipole contributions respectively.

VO_2 is a challenging material to integrate into patterned heterostructures, owing to the complexity of high deposition temperatures necessary to form the phase, and the multiple phases that are present in the V-O system. This requires a careful optimization of the device processing parameters to ensure film quality and preserving the desirable insulator-metal transition properties after the fabrication steps are completed. To fabricate the metasurface, we start with a 25 nm thin VO_2 layer deposited on quartz by magnetron sputtering from a V_2O_5 target under Ar/O_2 partial pressure. During deposition, the chamber was kept at 5 mtorr with a flow rate of 49 sccm Ar and 1 sccm 10% Ar balanced O_2. The oxygen partial pressure during deposition was therefore $2.67x10^{-4}$ Pa. As the utilized substrate (quartz) is not lattice-matched to VO_2, the deposition temperature has to be carefully adjusted in order to optimize the resulting crystallization and insulator to metal transition property of VO_2. The optimized deposition temperature found and used throughout this work was 750°C. As the transition properties of VO_2 may be altered by the subsequent plasma-based technological processes, we cover it with a thin passive layer. We therefore deposit a ~13 nm-thick SiO_2 layer on top of the VO_2 layer to protect it from the following technological steps. Note that this SiO_2 protective layer has only a negligible effect on the resulting optical properties of the devices as per our numerical simulations (see Fig. S6 in the Supporting Information). Next, we deposit a 240 nm-thick layer of amorphous Silicon (a-Si) by plasma-enhanced chemical vapor deposition using SiH_4 precursor at a temperature of 300°C. Hydrogen Silsesquioxane (HSQ) resist is then spun on the sample and patterned using E-beam lithography. After development in TMAH, the HSQ resist is used as a hard mask to transfer the patterns into a-Si via ICP-RIE dry etching with Cl_2/Ar. Finally, a 500-nm-thick layer of PMMA is spun on the sample. We systematically measured the optical properties of VO_2 by temperature-controlled ellipsometry after each technological process to verify that the insulator to metal properties remained unaffected. Each of the various fabrication steps listed above were optimized through a trial-and-error approach in order to preserve a fully functional VO_2 thin film in the final devices.

To measure the optical properties and VO_2-induced tunability of the metasurface, the sample is placed on a heat cell enabling ± 0.1°C temperature control. A broadband light source (halogen lamp) is focused on the devices through a 50× objective lens with 0.42NA and the light transmitted through the device is collected by a 50× objective lens with an iris diaphragm positioned at around the back focal plane to limit the collection angles to few degrees. Transmitted light is then dispersed in a spectrometer and detected with an InGaAs IR camera. The setup response is calibrated using an unpatterned part of the sample whose absolute reflection and transmission were measured via ellipsometry. Extinction spectra are computed as E=1-T. To measure the reversible tunability, the temperature is raised from 23°C to 100°C and back to room temperature. The heating-cooling cycle is repeated more than 10 times with no noticeable changes to the sample performance. A spectrum is collected every 5°C.

As presented in Figure 2 (c, d), the experimental transmission spectra are in very good agreement with the simulated spectra (Fig. 2 (a, b)) throughout the range of fabricated disks (all the experimental transmission spectra can be found in the Supporting Information, Fig. S3). We clearly distinguish the two separate modes, corresponding to ED and MD dipolar resonances in the range 550-580 nm, which subsequently overlap in the range 540-510 nm. When VO_2 is switched to its metallic state, the MD resonance (left branch) disappears, as expected from the theory and simulations.

In the following, we select two disks diameters (510 nm and 550 nm, respectively) to investigate in more details the consequence of overlapping ED-MD in the resulting modulation properties. In Fig. 3(a, b), we show the theoretical an experimental extinction spectra corresponding to insulator (40ºC) and metal (80ºC) phases of VO_2 layer for disks with diameters of 510 nm. At a wavelength of 1370 nm, the measured transmission contrast $T_{25°C}/T_{100°C}$ exceeds two orders of magnitude (see Fig. 4a for the contrast plot and Supporting Information for the transmission data visualized in logarithmic scale). On the other hand, for disks with diameter of 550 nm (Fig. 3 (e, f)), we experimentally observe a high extinction in the insulating state of VO_2, centered at 1450 nm, which is then spectrally shifted to about 1420 nm upon the VO_2 switch while still maintaining the high extinction regime. Importantly, unpatterned films with the same stack of layers neither present such suppressed transmissions nor a large transmission contrast between different states of VO_2 (see the corresponding spectra in the Supporting Information, Fig. S2)

Finally, in Figs. 4b, c we trace the measured transmission of both types of devices and observe a hysteresis behavior versus temperature. For the 510 nm disks, this hysteresis is observed clearly in the amplitude of transmission, while for the 550 nm disks, the hysteresis lies in the wavelength of high extinction. In the region 30ºC-70ºC the metasurface transmission can be in one of the two states depending on the history of heating-cooling cycle (see all experimentally measured spectra versus temperature during heating and cooling, in Fig. S4 of the Supporting Information). Therefore, our proposed platform may be used as an added feature to the recently proposed "field-programmable photonic meta-canvas"[44]: versatile devices could be written by optical means and, simply by maintaining the devices at modest temperatures (e.g. 70°C), the high-contrast metallic VO_2 regions can be kept over time and rapidly erased via a simple cool down process.[44]

In both cases, the reversible tuning of the metasurface properties is based on the redistribution of the electromagnetic energy between different multipoles of the dielectric disks (see the multipolar decomposition of the scattered fields Fig. 3 c,d and g,h), as well as a large modification of the absorption loss. In the following, we provide simplified explanations on the physics behind the different regimes of tunability. In the first functionality, showing a two-orders-of-magnitude contrast in the transmission, the Kerker's conditions are fulfilled in the insulating state and the device operates in the Huygens'-like metasurface regime even if not exactly at the resonance conditions. Upon the insulator-to-metal transition, the amplitude of the ED and MD resonances are strongly reduced and no longer overlap. The Kerker's condition is therefore broken. Simultaneously to that, the significant increase of the absorption loss upon the insulator to metal transition of VO_2 brings the metasurface close to the critical coupling conditions, in which the absorption loss equals the radiative loss resulting in a large increase in the overall optical absorption.

In the second functionality in which we demonstrate a spectrally tunable near-perfect absorber, the Kerker's condition holds in the insulating state but with a smaller amplitude than for the first functionality. Combined with the non-negligible absorption in the insulating VO_2, this translates into a near-zero transmission and a quasi-perfect absorption, hence a measured extinction higher than 0.95.

When VO_2 is switched to its metallic state both the ED and MD modes are blue-shifted. Their contributions, combined with the large increase in absorption result in a spectrally tuned near-perfect absorber. Most demonstrations of tunable absorbers reported so far only present either static tuning (i.e. adjusting the geometries in separate devices) or amplitude tuning (modulating the amount of absorbed light at a given wavelength).[6,41] We demonstrate here, the first active spectrally tunable absorber at telecom wavelength. Such active spectral tuning of absorption can find applications in dynamic refractive index sensing or tunable and frequency-selective detectors. We also envision the continuous tunability of such a device to be used as a "smart" actively reconfigurable notch filter to selectively block specific wavelengths from different tunable lasers or incoherent sources.

Even though this simplified picture disregards higher-order modes, it enables to grasp the physics at play behind this multifunctional reconfigurability in which we can both tune the amplitude and spectral properties of Mie resonances. This is further confirmed by full-wave numerical simulations that are in very good agreement with the experimental measurements (see Figs. 2 & 3).

Beyond this demonstration of multifunctional properties, this work provides a general framework to efficiently use the full complex refractive index tuning of VO_2, both for its refractive index modulation and optical absorption tuning. Importantly, the different effects shown could easily be shifted to other wavelengths by design, throughout the range of VO_2 tunability (near-IR to far-IR). This interplay between Mie resonances and the phase-change metamaterials uncovers a great potential of tunable dielectric metasurfaces for manipulating light in a rapid manner as the phase transition can be driven by fast light pulses,[45,46] paving the way to nanoscale optical switches, modulators, and sensors based on all-dielectric Mie-resonant metasurfaces.

Conclusion and Outlook

We have designed and tested experimentally, for the first time to our knowledge, a multifunctional reconfigurable platform based on Mie-resonant silicon metasurfaces tunable by a layer of phase-change material VO_2. The reversible and hysteretic tuning of the VO_2 state introduces two-orders-of-magnitude transmission contrast in the metasurface, and it can be tailored to produce a spectrally tunable near-perfect absorber. Novel technologies based on engineering of multipolar Mie resonances look promising for enhancing light-matter interactions creating resonant linewidths for tuning practical optical devices. Combining the advantages of the concepts of flat optics with a platform of all-dielectric metasurfaces incorporating VO_2 suggest novel strategies for tuning optical wavefronts with an electromagnetic field.

We believe our work will help to uncover a great potential of tunable dielectric metasurfaces to reconfigure optical wavefronts in a rapid manner, with the additional advantage of having hysteretic memory effects. It paves the way to nanoscale optical switches, modulators, neuromorphic photonics and sensors based on all-dielectric resonant metasurfaces.

Acknowledgements

The authors acknowledge financial support from the Australian Research Council (grant DP200101168), the Strategic Fund of the Australian National University, the French National Research Agency (ANR) under the project SNAPSHOT (ANR-16-CE24-0004) and AFOSR FA9550-18-1-0250. The authors acknowledge a support of the International Associated Laboratory in Photonics between France and Australia (LIA ALPhFA). AT, SK, and YK are indebted to J. Valentine for fruitful discussions.

Supporting Information

Complex refractive index variation of VO_2, transmission spectra for unpatterned and patterned layers, logscale plot of transmission spectra, influence of the SiO_2 spacer layer on optical properties. This material is available free of charge via the internet at http://pubs.acs.org.

References

(1) A. I. Kuznetsov, A. E. Miroshnichenko, M. L. Brongersma, Y. S. Kivshar, and B. Luk'yanchuk, "Optically resonant dielectric nanostructures," *Science* vol. 354, no. 6314, p. aag2472 (2016).

(2) S. S. Kruk and Y. S. Kivshar, "Functional Meta-Optics and Nanophotonics Governed by Mie Resonances," *ACS Photonics*, vol. 4, no. 11, pp. 2638–2649 (2017).

(3) S. M. Kamali, E. Arbabi, A. Arbabi, and A. Faraon, "A review of dielectric optical metasurfaces for wavefront control," *Nanophotonics* 7(6), 1041–1068 (2018).

(4) H. T. Chen, A. J. Taylor, and N. F. Yu, "A review of metasurfaces: physics and applications," *Rep. Prog. Phys.* 79(7),076401 (2016).

(5) A. M. Shaltout, V. M. Shalaev, and M. L. Brongersma, "Spatiotemporal light control with active metasurfaces," *Science* 364(6441), eaat3100 (2019).

(6) Q. He, S. L. Sun, and L. Zhou, "Tunable/Reconfigurable Metasurfaces: Physics and Applications," *Research* 2019,1–16 (2019).

(7) P. Gutruf, C. Zou, W. Withayachumnankul, M. Bhaskaran, S. Sriram, and C. Fumeaux, "Mechanically tunable dielectric resonator metasurfaces at visible frequencies," *ACS Nano*, vol. 10, no. 1, pp. 133–141, (2016).

(8) S. M. Kamali, E. Arbabi, A. Arbabi, Y. Horie, and A. Faraon, "Highly tunable elastic dielectric metasurface lenses," *Laser Photonics Rev.*, vol. 10, no. 6, pp. 1002–1008 (2016).

(9) A. Minovich, J. Farnell, D.N. Neshev, I. McKerracher, F. Karouta, J. Tian, D. A. Powell, I. V. Shadrivov, H.-H. Tan, C. Jagadish, and Y.S. Kivshar, "Liquid crystal based nonlinear fishnet metamaterials," *Appl. Phys. Lett.*, vol. 100, no. 12, p. 121113 (2012).

(10) A. Komar, Z. Fang, J. Bohn, J. Sautter, M. Decker, A. Miroshnichenko, T. Pertsch, I. Brener, Y. S. Kivshar, I. Staude, and D. N. Neshev, "Electrically tunable all-dielectric optical metasurfaces based on liquid crystals," *Appl. Phys. Lett.*, vol. 110, no. 7, p. 71109 (2017).

(11) T. Lewi, P. P. Iyer, N. A. Butakov, A. A. Mikhailovsky, and J. A. Schuller, "Widely tunable infrared antennas using free carrier refraction," *Nano Lett.*, vol. 15, no. 12, pp. 8188–8193 (2015).

(12) J. Park, J. Kang, S. J. Kim, X. Liu, and M. L. Brongersma, "Dynamic Reflection Phase and Polarization Control in Metasurfaces," *Nano Lett.*, vol. 17, no 1, p. 407-413 (2017).

(13) M. R. Shcherbakov, P. P. Vabishchevich, A. S. Shorokhov, K. E. Chong, D.-Y. Choi, I. Staude, A. E. Miroshnichenko, D. N. Neshev, A. A. Fedyanin, and Y. S. Kivshar, "Ultrafast all-optical switching with magnetic resonances in nonlinear dielectric nanostructures," *Nano Lett.*, vol. 15, no. 10, pp. 6985–6990 (2015).

(14) M. R. Shcherbakov, S. Liu, V. V. Zubyuk, A. Vaskin, P. P. Vabishchevich, G. Keeler, T. Pertsch, T. V. Dolgova, I. Staude, I. Brener, and A. A. Fedyanin, "Ultrafast all-optical tuning of direct-gap semiconductor metasurfaces," *Nat. Commun.*, 8, 17 (2017)

(15) D. Lencer, M. Salinga, B. Grabowski, T. Hickel, J. Neugebauer, and M. Wuttig, "A map for phase-change materials," *Nat. Mater.*, vol. 7, no. 12, pp. 972–977, (2008).

(16) A. Howes, Z. Zhu, D. Curie, J. R. Avila, V. D. Wheeler, R. F. Haglund, and J. G. Valentine, "Optical Limiting based on Huygens Metasurfaces" *Nano Lett.* 20, 6, 4638 (2020).

(17) M. Wuttig, H. Bhaskaran, and T. Taubner "Phase-change materials for non-volatile photonic applications". *Nat. Photonics*, 11(8), 465-476 (2017).

(18) Q. Wang, E.T.F. Rogers, B. Gholipour, C.-M. Wang, G. Yuan, J. Teng, and N. Zheludev, "Optically reconfigurable metasurfaces and photonic devices based on phase change materials" *Nat. Photonics* 10, 60-65 (2015).

(19) S. Abdollahramezani, O. Hemmatyar, H. Taghinejad, A. Krasnok, Y. Kiarashinejad, M. Zandehshahvar, A. Alù, and A. Adibi, "Tunable nanophotonics enabled by chalcogenide phase-change materials", *Nanophotonics* 9, 1189 (2020).

(20) S. Garcia-Cuevas Carrillo, G. R. Nash, H. Hasan, M. J. Cryan, M. Klemm, H. Bhaskaran, and C. D. Wright, "Design of practicable phase-change metadevices for near-infrared absorber and modulation applications," *Opt. Express* 24, 13563–13573 (2016).

(21) A. Karvounis, B. Gholipour, K. F. MacDonald, and N. I. Zheludev, "All-dielectric phase-change reconfigurable metasurface," *Appl. Phys. Lett.*109, 051103 (2016).

(22) C. Ruiz de Galarreta, A. M. Alexeev, Y.-Y. Au, M. Lopez-Garcia, M. Klemm, M. Cryan, J. Bertolotti, and C. D. Wright, "Nonvolatile reconfigurable phase-change metadevices for beam steering in the near infrared," *Adv. Funct. Mater.* 28, 1704993 (2018).

(23) C. R. de Galarreta, I. Sinev, A. M. Alexeev, P. Trofimov, K. Ladutenko, S. G.-C. Carrillo, E. Gemo, A. Baldycheva, J. Bertolotti, and C. D. Wright, "Reconfigurable multilevel control of hybrid all-dielectric phase-change metasurfaces," *Optica* 7(5), 476–484 (2020).

(24) S. Cueff, A. Taute, A. Bourgade, J. Lumeau, S. Monfray, Q. Song, P. Genevet, B. Devif, X. Letartre and L. Berguiga, "Reconfigurable Flat Optics with Programmable Reflection Amplitude Using Lithography-Free Phase-Change Material Ultra-Thin Films" *Adv. Opt. Mater.* 2001291 (2020).

(25) M. Julian, C. Williams, S. Borg, S. Bartram, and H. J. Kim, "Reversible optical tuning of GeSbTe phase-changemetasurface spectral filters for mid-wave infrared imaging," *Optica* 7(7), 746–754 (2020).

(26) M. Y. Shalaginov, S. An, Y. Zhang, F. Yang, P. Su, V. Liberman, J. B. Chou, C. M. Roberts, M. Kang, C. Rios, Q. Du,C. Fowler, A. Agarwal, K. Richardson, C. Rivero-Baleine, H. Zhang, J. Hu, and T. Gu, "Reconfigurable all-dielectric metalens with diffraction limited performance," *arXiv*:1911.12970 (2019).

(27) A. Leitis, A. Hessler, S. Wahl, M. Wuttig, T. Taubner, A. Tittl, and H. Altug,"All-dielectric programmable Huygens' metasurfaces," *Adv. Funct. Mater.* 30, 1910259 (2020).

(28) J. Rensberg, S. Zhang, Y. Zhou, A. S. McLeod, C. Schwarz, M. Goldflam, M. K. Liu, J. Kerbusch, R. Nawrodt, S. Ramanathan, D. N. Basov, F. Capasso, C. Ronning, and M. A. Kats, "Active Optical Metasurfaces

Based on Defect-Engineered Phase-Transition Materials," *Nano Lett.* 16(2), 1050–1055 (2016).
(29) N. A. Butakov, I. Valmianski, T. Lewi, C. Urban, Z. Ren, A. A. Mikhailovsky, S. D. Wilson, I. K. Schuller, and J. A. Schuller, "Switchable plasmonic–dielectric resonators with metal–insulator transitions," *ACS Photonics* 5(2), 371–377 (2018).
(30) S. Cueff, D. Li, Y. Zhou, F. J. Wong, J. A. Kurvits, S. Ramanathan, and R. Zia, "Dynamic control of light emission faster than the lifetime limit using VO_2 phase-change," *Nat. Commun.* 6, 8636 (2015).
(31) Y. Kim, P. C. Wu, R. Sokhoyan, K. Mauser, R. Glaudell, G. K. Shirmanesh, and H. A. Atwater, "Phase modulation with electrically tunable vanadium dioxide phase-change metasurfaces," *Nano Lett.* 19(6), 3961–3968 (2019).
(32) O. L. Muskens, L. Bergamini, Y. Wang, J. M. Gaskell, N. Zabala, C. H. de Groot, D. W. Sheel, and J. Aizpurua, "Antenna-assisted picosecond control of nanoscale phase transition in vanadium dioxide," *Light: Sci. Appl.* 5(10), e16173 (2016).
(33) S. K. Earl, T. D. James, D. E. Gómez, R. E. Marvel, R. F. Haglund, Jr., and A. Roberts, "Switchable polarization rotation of visible light using a plasmonic metasurface," *APL Photonics* 2, 016103 (2017)
(34) Z. Shao, X. Cao, H. Luo, and P. Jin, "Recent progress in the phase-transition mechanism and modulation of vanadium dioxide materials," *NPG Asia Mater.*, vol. 10, no. 7. pp. 581–605 (2018).
(35) S. Cueff, J. John, Z. Zhang, J. Parra, J. Sun, R. Orobtchouk, S. Ramanathan, and P. Sanchis, "VO_2 nanophotonics", *APL Photonics* 5, 110901 (2020).
(36) S. Kruk, J. John, Z. Zhang, H. S. Nguyen, L. Berguiga, P. Rojo Romeo, R. Orobtchouk, S. Ramanathan, Y. Kivshar & S. Cueff, "Tunable Mie-resonant dielectric metasurfaces based on VO_2 phase-change materials". In *CLEO: QELS_Fundamental Science* (pp. FTh3Q-4) (2020).
(37) M. Decker, I. Staude, M. Falkner, J. Dominguez, D. N. Neshev, I. Brener, T. Pertsch, and Y. S. Kivshar, "High-efficiency dielectric Huygens' surfaces," *Adv. Opt. Mater.* 3(6), 813–820 (2015).
(38) R. Alaee, M. Albooyeh, and C. Rockstuhl, "Theory of metasurface based perfect absorbers," *J. Phys. D* 50, 503002 (2017).
(39) Y. Cui, Y. He, Y. Jin, F. Ding, L. Yang, Y. Ye, S. Zhong, Y. Lin, and S. He, "Plasmonic and metamaterial structures as electromagnetic absorbers," *Laser Photonics Rev.* 8(4), 495–520 (2014).
(40) M. Kerker, D.S. Wang and L. Giles, "Electromagnetic scattering by magnetic spheres" *J. Opt. Soc. Am.* 73,765–767 (1983).
(41) X. Liu, K. Fan, I. V. Shadrivov, and W. J. Padilla, "Experimental realization of a terahertz all-dielectric metasurface absorber," *Opt. Express*, vol. 25, no. 1, p. 191 (2017).
(42) J. John, Y. Gutierrez, Z. Zhang, H. Karl, S. Ramanathan, R. Orobtchouk, F. Moreno, and S. Cueff, "Multipolar resonances with designer tunability using VO_2 phase-change materials," *Phys. Rev. Appl.* 13, 044053 (2020).
(43) R. Alaee, C. Rockstuhl and I. Fernandez-Corbaton, "Exact Multipolar Decompositions with Applications in Nanophotonics," *Adv. Opt. Mater.*, vol. *7*, no. 1. (2019).
(44) K. Dong, S. Hong, Y. Deng, H. Ma, J. Li, X. Wang, J. Yeo, L. Wang, S. Lou, K. B. Tom, K. Liu, Z. You, Y. Wei, C. P. Grigoropoulos, J. Yao, J. Wu, "A lithography-free and field-programmable photonic metacanvas," *Adv. Mater.* 30, 1703878 (2018).
(45) A. Cavalleri, C. Tóth, C. W. Siders, J. A. Squier, F. Ráksi, P. Forget, and J. C. Kieffer, "Femtosecond structural dynamics in VO_2 during an ultrafast solid-solid phase transition," *Phys. Rev. Lett.* 87(23), 237401 (2001).
(46) K. A. Hallman, K. J. Miller, A. Baydin, S. M. Weiss, and R. F. Haglund, "Sub-Picosecond Response Time of a Hybrid VO_2: Silicon Waveguide at 1550 nm." *Adv. Opt. Mater.*, 2001721 (2020).

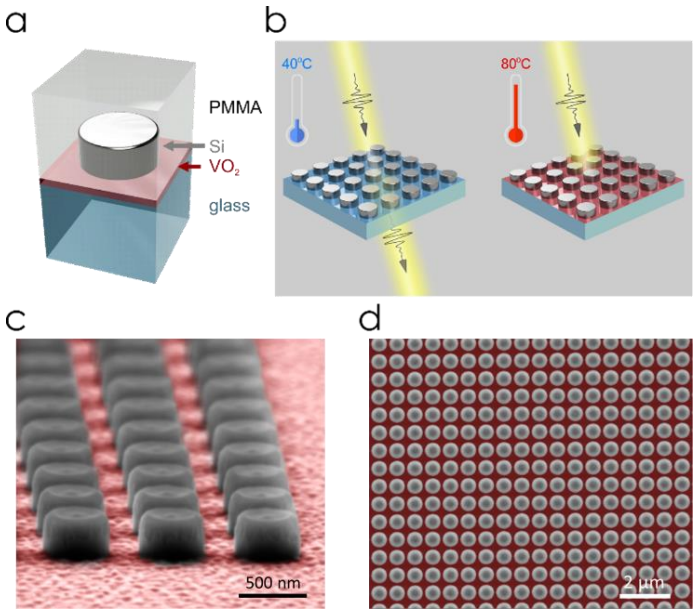

Fig. 1. Tunable dielectric metasurfaces. (a) Design concept: a silicon meta-atom is embedded into glass/PMMA surrounding with a buried thin VO_2 layer of 25 nm. Si disk height: 240 nm, disk radius: 255 nm, square lattice period: 700 nm, PMMA layer thickness: 500 nm. (b) Functionality of the metasurface featuring tunable extinction with temperature variation. (c, d) Electron microscope images of the fabricated Si-VO_2 metasurface prior to the PMMA coating (VO_2 layer in false red color).

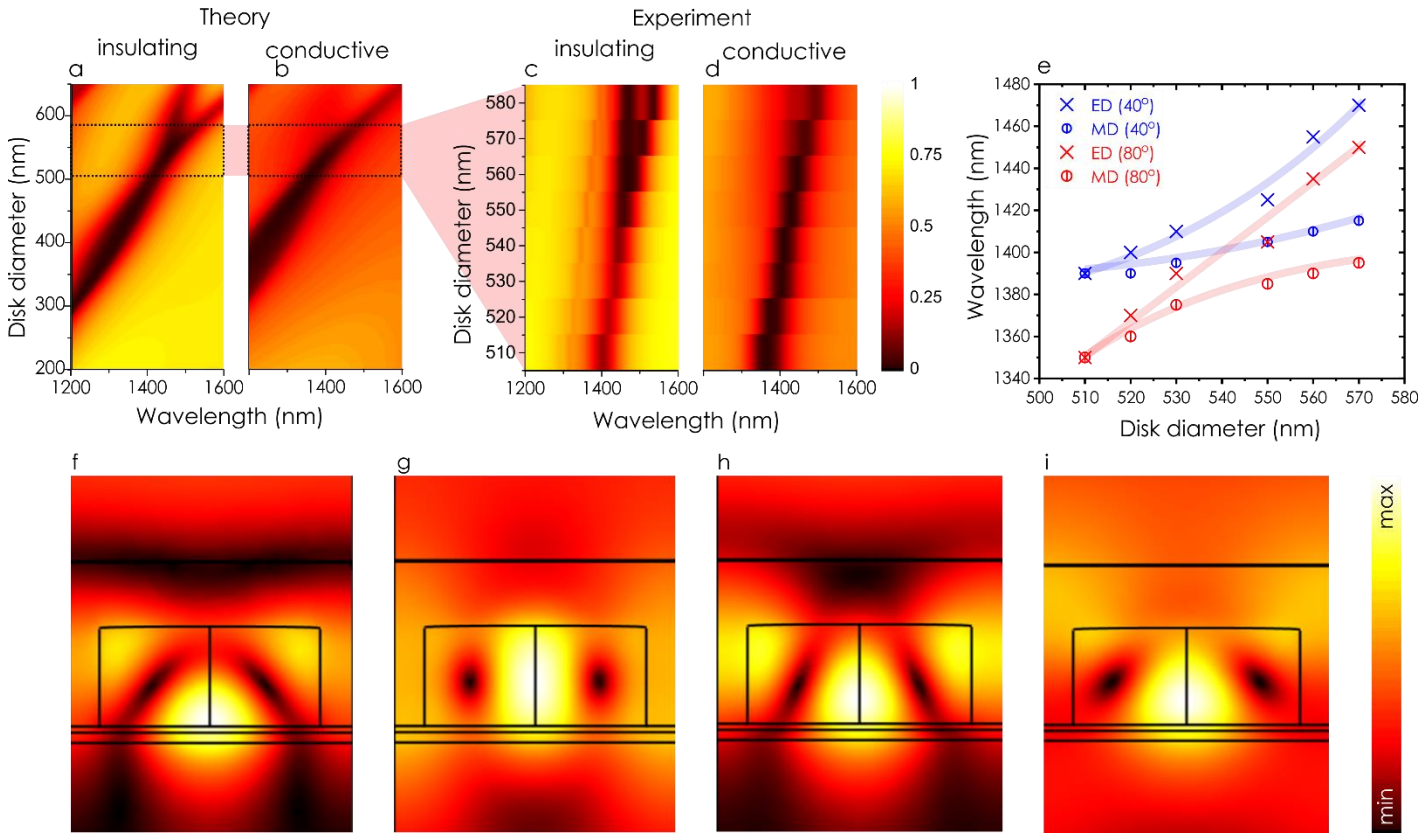

Fig. 2. Experimental and theoretical optimization of the metasurfaces. (a,b) Calculated and (c,d) experimentally measured transmission spectra of the metasurfaces with varying disk diameter for the (a,c) insulating and (b,d) conductive phases of the VO_2 layer. (e) Theoretically calculated maxima of the electric dipole and the magnetic dipole Mie resonances for metasurfaces with varying disk diameters in (blue) insulating and (red) conductive phases. Lines are guides for an eye. (f-i) Normalized electric field distribution in the cross-sections of the hybrid a-Si/VO_2 nanodisks 550 nm in diameter when VO_2 is insulating (f,g) and metallic (h,i) for wavelengths 1410 nm (f) and 1380 nm (h) at the magnetic dipole maximum as per Fig. 2e and for wavelengths 1470 nm (g) and 1450 nm (i) at the electric dipole maximum as per Fig 2e (g,i).

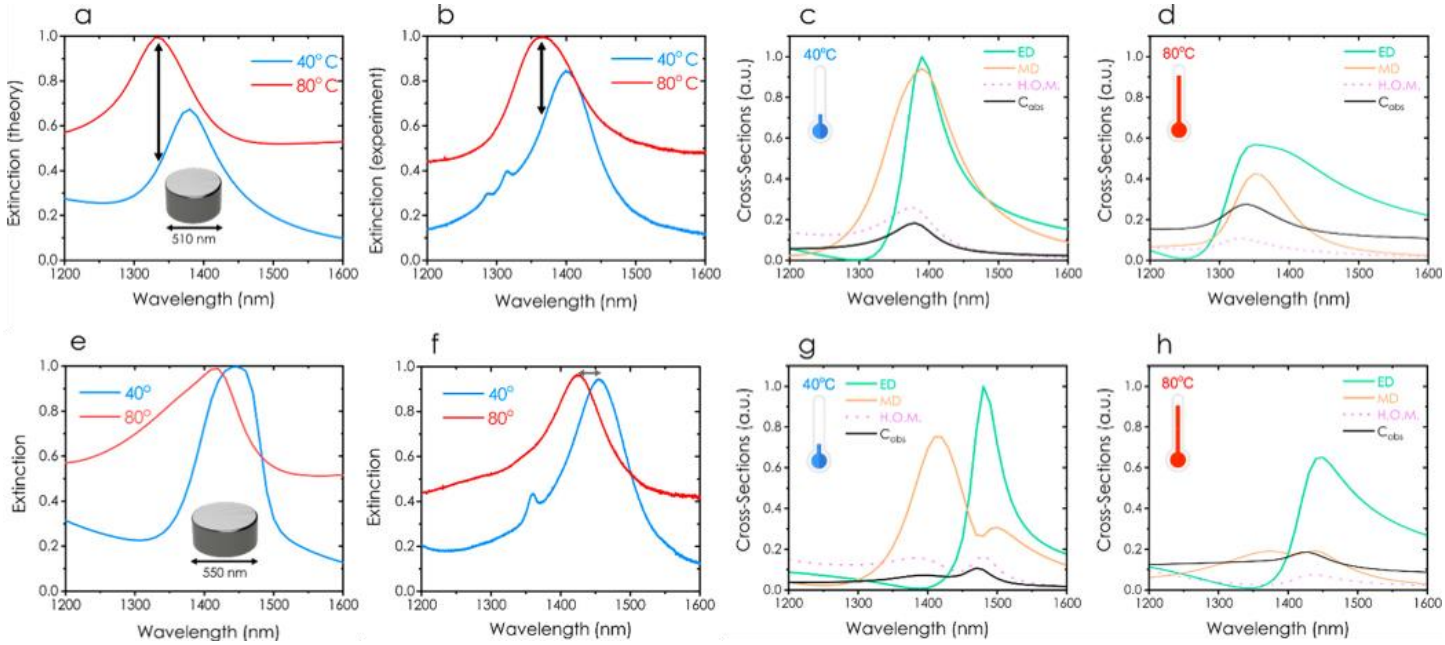

Fig. 3. Experimental vs theoretical results on tunability of the Si-VO_2 metasurface. (a-d) Theoretical extinction (a), experimental extinction (b), absorption and scattering characteristics (c,d) of optical resonances for disks with a diameter of 510 nm in the two states of VO_2: insulating (c) and metal (d). The scattering component of the extinction is presented as a decomposition of Mie multipoles. (e-h) Theoretical extinction (e), experimental extinction (f), absorption and scattering (g,h) of optical resonances for disks with a diameter of 550 nm in the two states of VO_2: insulating (g) and metal (h). H.O.M.: higher-order multipoles.

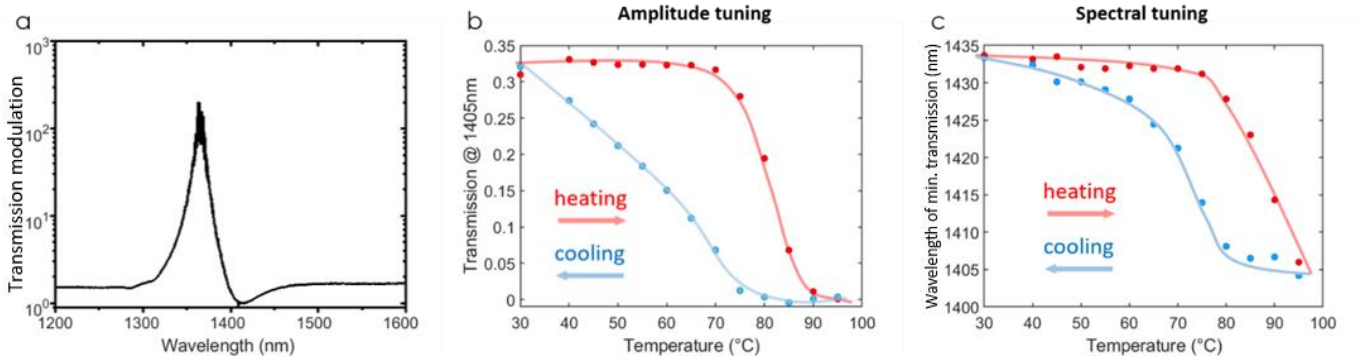

Fig. 4. Experimental large transmission modulation, spectral tuning and hysteretic memory effect of the Si-VO_2 metasurface. (a) Two orders of magnitude experimentally measured transmission contrast ($T_{25°C}/T_{100°C}$) induced by the VO_2 insulator to metal transition on the metasurface with disk's diameter of 510 nm (b) Reversible tuning of the amplitude of transmission featuring a hysteresis behavior of the same device. (c) Reversible spectral tuning of the metasurface transmission showing a continuously reconfigurable near-perfect absorber (metasurface with disk's diameter of 550 nm.)

TOC Graphic

For Table of Contents Use Only

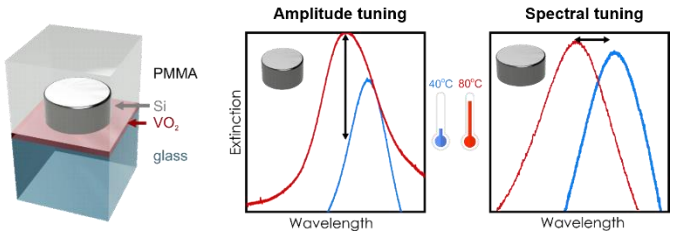

Title: Tunable Mie-resonant dielectric metasurfaces based on VO_2 phase-transition materials

Authors: Aditya Tripathi, Jimmy John, Sergey Kruk, Zhen Zhang, Hai Son Nguyen, Lotfi Berguiga, Pedro Rojo Romeo, Régis Orobtchouk, Shriram Ramanathan, Yuri Kivshar and Sébastien Cueff

Synopsis: Mie-resonant silicon-based metasurfaces tunable via the insulator-to-metal transition of a thin VO_2 layer, showing amplitude tuning and spectral tuning of optical extinction.